Mixing efficiency in an excitable medium with chaotic shear flow

Vicente Pérez-Muñuzuri* and Guillermo Fernández-García
Group of Nonlinear Physics, Faculty of Physics, University of Santiago de Compostela, E-15782 Santiago de Compostela, Spain
(Received 16 November 2006; revised manuscript received 23 January 2007; published 16 April 2007)

The effect of a time-periodic chaotic shear flow on an excitable chemical medium is studied numerically. Stirring effects on pattern formation strongly depend on the shear amplitude and the ratio of the advective and chemical time scales (Damköhler number, Da). We have observed that the wave period increases with decreasing Da below some critical value, afterwards the period decreases until complete wave annihilation. In the last case, before final extinction, a set of uncorrelated, nonstationary excitable dots survive, whose number depends on the mixing rate. Insights on the nature of this critical behavior are obtained through the calculation of the mixing efficiency of the flow.

DOI: 10.1103/PhysRevE.75.046209 PACS number(s): 82.40.Bj, 47.54.−r, 47.70.Fw, 82.40.Ck

I. INTRODUCTION

Many theoretical [1] and experimental [2] studies have investigated the effects of stirring on nonlinear chemical media, especially under batch conditions on a continuously stirred tank reactor (CSTR), and have shown that a spatially distributed system may behave completely different from its homogeneous reference system. It is often assumed that increasing stirring leads to spatial homogenization through a rapid increase of the overall oscillation period of the medium. However, imperfectly mixed environments are common characteristics of many real chemical and biological processes (see Refs. [3,4] and references therein). The presence of heterogeneities can be rapidly amplified in a nonlinear chemical environment, and survive, even under strong mixing conditions.

Excitable media display a very rich spatiotemporal behavior with regimes ranging from fairly well ordered structures of propagating waves [5] to highly uncorrelated spatiotemporal chaos. Since long ago, propagation of waves in excitable media has been studied mostly in the framework of chemistry and biology. More recently, the combined effects of reaction, diffusion, and advection have become an area of active research [6,7].

The aim of this paper is to study the spatiotemporal pattern formation in a system driven by a nonlinear chemical dynamics corresponding to an excitable chemical reaction under the presence of chaotic flows. For mixing rates below final extinction of the excitable wave fronts, mixing efficiency is not equally distributed through the medium giving rise to an ensemble of single nonstationary excited dots that vibrate with a frequency proportional to the stirring rate. For time-periodic flows, the mixing process is a combination of stirring, stretching, and folding, which generates intricate structures with wide distributions of length scales that span several orders of magnitude, even for large mixing strength. The length scale distributions characterizing such structures control the rates of diffusional homogenization and the rate of reactions taking place at small scales of the flow. Thus, some excited dots can survive to the homogenization for large stirring values. To that end, in this paper we have used a *sinusoidal chaotic shear flow* [8,9] to study pattern formation under two different scenarios: (i) for slow fluid mixing, wave fronts propagate through the medium, become distorted due to the shear flow, and their wave period increases with Da; and (ii) for mixing rates above some critical value and below final extinction, nonstationary excited dots survive whose number and oscillation rate depend on the mixing efficiency.

II. MODEL

The full model is defined by

$$\frac{\partial \mathbf{C}}{\partial t} + (\mathbf{V}\cdot\boldsymbol{\nabla})\mathbf{C} = \mathbf{F}(\mathbf{C}) + D\nabla^2\mathbf{C}. \tag{1}$$

Here, $\mathbf{C}=[u,v]$ and $\mathbf{F}=[F_u,F_v]$ is the nonlinear chemical excitable dynamics represented by the two-variable Oregonator model [10],

$$F_u = \frac{1}{\varepsilon}\left(u - u^2 - (fv+\phi)\frac{u-q}{u+q}\right),$$

$$F_v = u - v, \tag{2}$$

where u and v are the dimensionless concentrations of $HBrO_2$ and the catalyst, respectively. f is a parameter related to the kinetics of the Belousov-Zhabotinsky reaction. q and ε are scaling parameters, and ϕ is the bromide flow due to photochemical effects. The excitability of the medium is measured in terms of $1/\varepsilon$. The diffusion matrix is diagonal with coefficients $(D,0)$.

The velocity field is modeled by a two-dimensional time-periodic flow capable of producing repeated stretching and folding of fluid parcels, a common characteristic of chaotic mixing (Fig. 1). Thus, the velocity field $\mathbf{V}=[V_x,V_y]$ consists of a *periodic shear flow* [8,9] given by

*Electronic address: vicente.perez@cesga.es

$$(V_x, V_y) = \left(\frac{AL}{T_f}\sin(2\pi y + \varphi_n), 0\right), \quad nT_f \le t < \left(n + \tfrac{1}{2}\right)T_f,$$

$$(V_x, V_y) = \left(0, \frac{AL}{T_f}\sin(2\pi x + \varphi_{n+1})\right), \quad \left(n + \tfrac{1}{2}\right)T_f \le t < (n+1)T_f. \tag{3}$$

T_f and A are the period and shear amplitude of the flow, respectively [11], n is the number of periods, and t is the time. This velocity field is assumed to be independent of the concentration vector $\mathbf{C}$. For the discussion below, it is interesting to rescale the model equations [4,9] by measuring time in units of T_f, $\bar{t}=t/T_f$, length in units of L, $\bar{\mathbf{r}}=\mathbf{r}/L$, $\mathbf{r}=(x,y)$, and velocity as $\bar{\mathbf{V}}=\mathbf{V}/U_0$, $U_0=L/T_f$. This leads to the equations, on dropping the bars for convenience,

$$\frac{\partial u}{\partial t} + (\mathbf{V}\cdot\boldsymbol{\nabla})u = \mathrm{Da}\, F_u + \mathrm{Pe}^{-1}\nabla^2 u,$$

$$\frac{\partial v}{\partial t} + (\mathbf{V}\cdot\boldsymbol{\nabla})v = \varepsilon\, \mathrm{Da}\, F_v, \tag{4}$$

where

$$\mathrm{Da} = T_f/\varepsilon, \quad \mathrm{Pe} = L^2/DT_f \tag{5}$$

are the Damköhler and Péclet dimensionless numbers. Da measures the ratio of the advective and chemical time scales and Pe gives the ratio between the advective and diffusive transport. Large Damköhler numbers imply that the reaction is very fast on the time scale of advection, while for small values of Da, the reaction is slower than advection.

The reaction-advection-diffusion problem was integrated on a $L\times L$ square lattice using an implicit method for advection and diffusion (spatial step size $\Delta=1$) with a fourth-order Runge-Kutta with time step $\Delta t=0.001$ for the time integration of the local chemical dynamics. Periodic boundary conditions are imposed for the concentration gradients. Random initial conditions are set for the concentration field, and the flow was switched on after a spin-up of $t=200$ t.u. (where t.u. denotes time units). Results below are independent of the initial random condition and the spin-up period. In the absence of advection, the resulting pattern is a train of wave fronts with wave period T_0. The model (2)–(4) is investigated for different periods T_f and shear amplitudes A of the flow. The influence of the excitability on the obtained results is also studied.

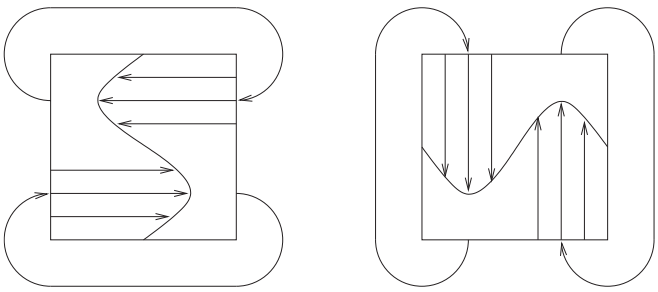

FIG. 1. Sketch of the shear flow, which takes place on a square box with periodic boundary conditions. The flow is the combination of two orthogonal motions, each with a sinusoidal velocity profile. Each motion acts alternatively for one-half of a flow period.

III. RESULTS

The effect of the periodic shear flow on the chemically excitable medium described by the Oregonator kinetics is shown in Fig. 2. As the forcing frequency of the flow $\nu_f = 1/T_f$ increases (keeping constant the shear amplitude A), the resulting pattern moves from a periodic wave train to an uncorrelated, noncoherent, set of excitable nonstationary dots. Successive folding and stretching of fluid parcels increase with stirring ν_f leading to fronts breakup. Annihilation of some parts of the waves takes place only if a sufficiently large amount of the inhibitor accumulates in front of the

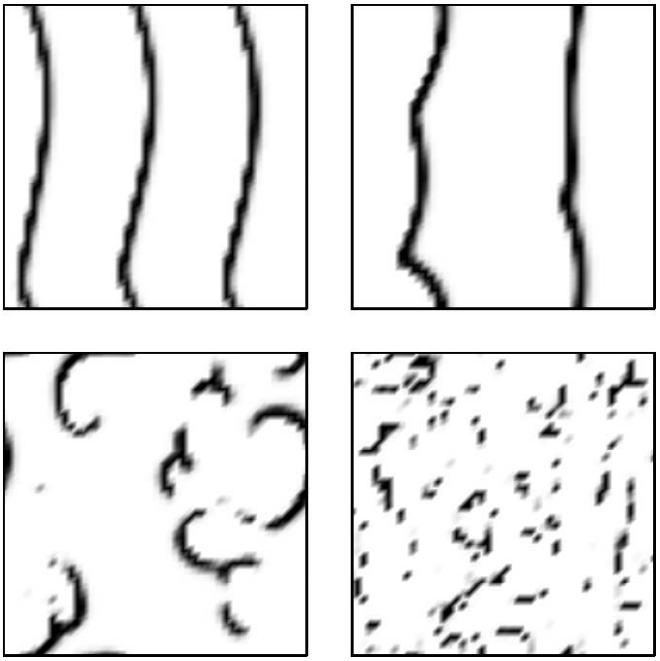

FIG. 2. Sequence of u fields for different values of the forcing frequency ν_f for the periodic shear flow. From left to right and from top to bottom plots: $\log_{10}\nu_f=-1.0$ (Da=200), $\log_{10}\nu_f=-0.5$ (Da=63), $\log_{10}\nu_f=-0.25$ (Da=35), and $\log_{10}\nu_f=0.25$ (Da=11), respectively. Set of parameters: $A=3.4$, $f=3$, $\varepsilon=0.05$, $q=0.002$, $\phi=0.002$, $D=1$, and $L=50$. For these parameters, the model is excitable and the wave period $T_0\approx 4.2$ t.u.

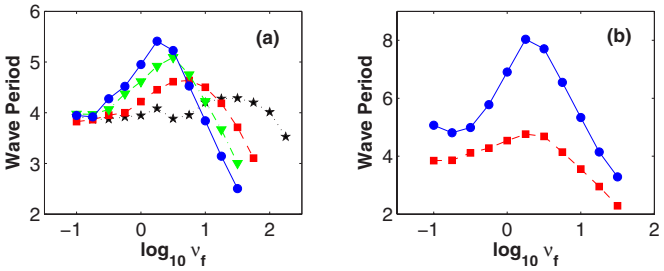

FIG. 3. (Color online) Mean wave period as a function of the forcing frequency ν_f for different values of the shear amplitude A (a) and excitability $1/\varepsilon$ (b). Wave periods are defined as the minimum distance between two consecutive u-peaks. Periods were calculated at each grid point of the lattice and a distribution of periods was obtained as time goes on. Then, a mean value was calculated. (a) Circles, $A=3.4$; triangles, $A=2.4$; squares, $A=1.4$; and stars, $A=0.4$ $(1/\varepsilon=20)$. (b) Circles, $1/\varepsilon=16$, and squares, $1/\varepsilon=22$ $(A=3.4)$. The rest of the parameters are the same as in Fig. 2.

excitation wave. In this sense, increasing the shear amplitude also favors this mechanism and planar wave fronts breakup occurs at smaller frequency values. After breakup, wave front ends tend to curl and spiral waves develop, which once again are affected by the periodic shear flow and new breaks occur, and so successively. Finally, for large forcing frequencies only some excited points remain. This behavior is similar to others observed in chemical excitable media under the effect of alternating electric fields [12]. Then, the electric field played the role of a periodic advective field but only acting in one direction. Here, the periodic shear flow is capable of producing repeated stretching of fluid elements, a common characteristic of any chaotic advection.

In order to characterize the behavior of the chemical media, the mean wave period T is shown in Fig. 3(a) as a function of the forcing frequency for different shear amplitudes. For all values of A, the wave period reaches a maximum value at $\nu_f=\nu_{\mathrm{mix}}$. This value moves toward lower values with increasing shear amplitude. The nature of this behavior will be explained below in terms of the mixing efficiency of the flow. As a consequence of the Damköhler number (5) multiplying the chemical dynamics, for $\nu_f<\nu_{\mathrm{mix}}$, the wave period increases with the forcing frequency. Period enhancement is, as well, monotonously increasing with the shear amplitude.

The rate of period enhancement is studied in terms of the excitability of the medium $1/\varepsilon$ [Fig. 3(b)]. For this purpose, the dimensionless parameter *looseness* [12], defined as the ratio between the period of the wave and the refractory period of the medium, can be used as a measure of the minimum time needed by a point to be reexcited after the passage of a previous wave. As the excitability of the medium is increased, looseness decreases and consecutive waves propagate closer to each other with smaller amplitude which favors wave fronts breakup. Then, planar wave fronts break at smaller shear amplitudes and frequencies but the value of ν_{mix} remains the same. Period enhancement with mixing is larger for smaller excitability but, in general, wave period decrease with increasing excitability (or increasing Da) as the reaction becomes faster than the advective field.

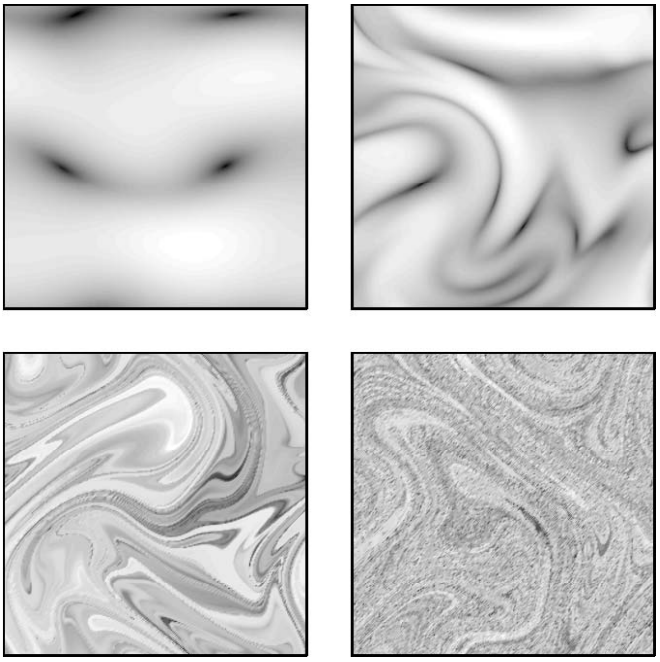

FIG. 4. Sequence of finite-time Lyapunov exponent (FTLE) fields for different values of the forcing frequency ν_f. The exponent grows from darker to lighter regions of the pattern. 62 500 Lagrangian particles were used in the simulations. The parameters are the same as in Fig. 2.

For $\nu_f>\nu_{\mathrm{mix}}$, the behavior is completely different, initial wave fronts are successively stretched and folded periodically, as before, but now without time to recover themselves to their original shape, fronts are annihilated. Only in those places where the mixing efficiency is small, some excited dots survive whose number depends on their width and mixing rate. Increasing the diffusion, wave fronts become wider and more difficult to be broken. Only a small fraction of excited dots can survive as the diffusion length $\sqrt{T_f D}$ increases and larger areas of the lattice characterized by a small mixing efficiency are needed now. In this case, increasing diffusion favors an earlier homogenization. These excited dots vibrate with a mean frequency $1/T$ that increases linearly with both the shear amplitude and the forcing frequency, as

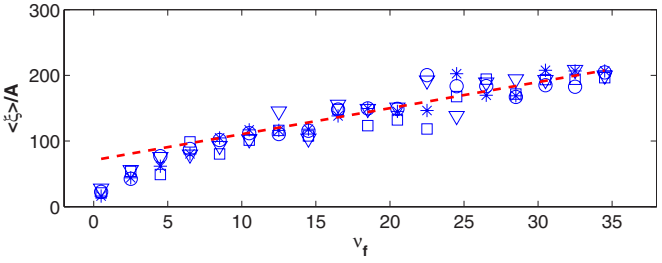

FIG. 5. (Color online) Plot of the spatial average mixing efficiency normalized by the forcing amplitude, $\langle\xi\rangle/A$, as a function of the forcing frequency ν_f. The dashed line is the linear fit of the numerical data for $\nu_f>\nu_{\mathrm{mix}}$ $(\langle\xi\rangle\sim A\nu_f)$. Data symbols are the same as in Fig. 3.

$$1/T \approx mA\nu_f + 1/T_0, \tag{6}$$

where T_0 is the wave period of the chemical medium without advection, and m is a fitting constant that increases with the excitability of the medium. Equation (6) indicates that dots vibrate faster for larger values of A and consequently smaller values of ν_f will be needed to annihilate the remnant dots before the medium could be considered to be completely mixed (i.e., no excited points remain in the medium). Note in Fig. 3(a) that curves end earlier for larger A indicating that no periods were measured or patterns observed afterwards.

Insight into the pattern formation and the observed wave periods maxima can be gained by calculating fields of the finite-time Lyapunov exponent (FTLE) [13] $\lambda(t) = (1/t)\ln[d(t)/d(0)]$, where $d(t)$ is the distance among two tracers, initially separated by $d(0)$, at time t. FTLE accounts for the integrated effect of the flow because it is derived from particle trajectories, and thus is indicative of the actual transport behavior. Figure 4 shows the Lyapunov exponents calculated for the same parameters as in Fig. 2. In average, the mean FTLE increases with the mixing frequency, so the time needed to separate two fluid parcels decreases with increasing ν_f. In other words, the mixing efficiency $\xi(t)$ defined by the ratio $d(t)/d(0)$ increases with ν_f (Fig. 5). Regions where the FTLE is large are those where filaments are stretched in one direction and thinned in an orthogonal direction; i.e., these are the regions where advection and diffusion best mix the contents of the fluid and any excited front crossing that region will be slowed down or annihilated. For small forcing frequencies, large coherent regions form which can be followed in space and time; they are translated and deformed by the flow but conserve identity and do not disappear upon further mixing. In this case, wave fronts can be broken, but still large front pieces can be observed. Then, best mixing will be obtained when these large coherent regions mix up completely or at least they approach to that ($\lambda's$ variance tends to zero), and the FTLE pattern approaches a fractal set. For the parameters of the simulation, this optimal value ν_{mix} can be attained as the minimum frequency such that the mixing efficiency scales as $\mathrm{Pe} \sim \nu_f$ (Fig. 5), the classical scaling derived by the simplest eddy diffusion theory [14]. Then, ν_{mix} bounds from below the range of forcing frequencies for which the excited dots oscillate at a rate proportional to the mixing efficiency ($1/T \sim \xi \sim A\nu_f$).

IV. CONCLUSIONS

We have observed two different behaviors for pattern formation as mixing increases. In the first case, wave period increases with decreasing Da as expected. The rate of period enhancement increases with the shear amplitude. Similar results have also been observed in the literature [2,9,15] under different types of flows and/or active media. On the other hand, for values of ν_f larger than some critical value ν_{mix}, no waves were observed, but a set of excited dots spread through the lattice whose oscillation period decreases with decreasing Da. Then, full homogenization can be attained for larger shear amplitudes but smaller frequencies. It is also noticeable the similarity of the structures here found with localized structures in reaction-diffusion systems, also called *oscillons* [16]. In that case, structures remain localized but almost stationary with time with just some periodic modulation of their size and are believed to be the experimental evidence of the coupling between Hopf and Turing modes. In our present case, the structures remain shape-constant, but oscillate with the frequency imposed externally and they move with the flow, thus, remain stationary in a moving frame of reference. In such a sense, a similarity can be established although, now, the Turing-type instability is induced by convection (like the FDS structures) [17]. More recently, similar localized spots have been observed numerically in a bistable chemical model forced by a periodic shear flow where the Da number is great enough to sustain a disturbance, but not as great as to lead to a global homogeneous state [18].

We expect our results to be valid for any excitable medium force with a time-periodic chaotic flow. The processes observed here giving rise to successive wave fronts breakup and period increasing are general to any reaction-diffusion-advection model where the Da number multiplies the reaction term. Besides, as chaotic advection develops, only excited dots can survive at places of the lattice where mixing efficiency is smaller than in neighboring places. Experimentally, similar results should be observed for setups where large ranges of Da numbers and low values of the diffusion (large Péclet numbers) could be attained.

ACKNOWLEDGMENT

This work was supported by Ministerio de Educación y Ciencia under Research Grant No. FIS2004-03006.

[1] J. A. Aronovitz and D. R. Nelson, Phys. Rev. A **29**, 2012 (1984); J. Boissonade and P. DeKepper, J. Chem. Phys. **87**, 210 (1987); P. Ruoff, J. Phys. Chem. **97**, 6405 (1993).

[2] I. Nagypal and I. R. Epstein, J. Chem. Phys. **89**, 6925 (1988); M. Menzinger and A. K. Dutt, J. Phys. Chem. **94**, 4510 (1990); L. López-Tomás and F. Sagués, *ibid.* **95**, 701 (1991); F. Ali and M. Menzinger, *ibid.* **96**, 1511 (1992); V. K. Vanag and D. P. Melikhov, *ibid.* **99**, 17372 (1995).

[3] J. M. Ottino, *The Kinematics of Mixing* (Cambridge University Press, Cambridge, 1989).

[4] T. Tél, A. de Moura, C. Grebogi, and G. Károlyi, Phys. Rep. **413**, 91 (2005).

[5] *Chemical Waves and Patterns*, edited by R. Kapral and K. Showalter (Kluwer Academic, Dordrecht, 1993).

[6] C. R. Nugent, W. M. Quarles, and T. H. Solomon, Phys. Rev. Lett. **93**, 218301 (2004); M. S. Paoletti, C. R. Nugent, and T. H. Solomon, *ibid.* **96**, 124101 (2006); V. Pérez-Muñuzuri, Phys. Rev. E **73**, 066213 (2006).

[7] Z. Neufeld, Phys. Rev. Lett. **87**, 108301 (2001); C. Zhou, J. Kurths, Z. Neufeld, and I. Z. Kiss, *ibid.* **91**, 150601 (2003).

[8] M. M. Alvarez, F. J. Muzzio, S. Cerbelli, A. Adrover, and M. Giona, Phys. Rev. Lett. **81**, 3395 (1998).

[9] I. Z. Kiss, J. H. Merkin, and Z. Neufeld, Phys. Rev. E **70**, 026216 (2004).

[10] H. J. Krug, L. Pohlmann, and L. Kunhert, J. Phys. Chem. **94**, 4862 (1990); I. Sendiña-Nadal, S. Alonso, V. Pérez-Muñuzuri, M. Gómez-Gesteira, V. Pérez-Villar, L. Ramírez-Piscina, J. Casademunt, J. M. Sancho, and F. Sagués, Phys. Rev. Lett. **84**, 2734 (2000).

[11] Transport barriers due to Kolmogorov-Arnold-Moser (KAM) tori, typically present in periodically driven conservative flows, can be avoided by breaking the periodicity using a random phase φ, that is selected independently and uniformly from $[0,2\pi)$ in each half of the period.

[12] J. J. Taboada, A. P. Muñuzuri, V. Pérez-Muñuzuri, M. Gómez-Gesteira, and V. Pérez-Villar, Chaos **4**, 519 (1994).

[13] V. Artale, G. Boffetta, A. Celani, M. Cencini, and A. Vulpiani, Phys. Fluids **9**, 3162 (1997); G. Lapeyre, Chaos **12**, 688 (2002).

[14] C. R. Doering and J. L. Thiffeault, Phys. Rev. E **74**, 025301(R) (2006).

[15] J. Nolen and J. Xin, Multiscale Model. Simul. **1**, 554 (2003).

[16] D. G. Míguez, S. Alonso, A. P. Muñuzuri, and F. Sagués, Phys. Rev. Lett. **97**, 178301 (2006).

[17] M. Kaern, R. Satnoianu, A. P. Muñuzuri, and M. Menzinger, Phys. Chem. Chem. Phys. **4**, 1315 (2002).

[18] S. M. Cox, Phys. Rev. E **74**, 056206 (2006).